



Published in final edited form as:

*Appl Spectrosc.* 2010 October ; 64(10): 1160–1166. doi:10.1366/000370210792973604.

## Nondestructive Assessment of Engineered Cartilage Constructs Using Near-Infrared Spectroscopy

DORUK BAYKAL, ONYI IRRECHUKWU, PING-CHANG LIN, KATE FRITTON, RICHARD G. SPENCER, and NANCY PLESHKO\*

Drexel University, Philadelphia, Pennsylvania 19104 (D.B.); National Institute on Aging, NIH, Baltimore, Maryland 21224 (O.I., P.-C.L., R.G.S.); Exponent, Inc., Philadelphia, Pennsylvania 19104 (K.F.); and Temple University, Philadelphia, Pennsylvania 19122 (N.P.)

### Abstract

Noninvasive assessment of engineered cartilage properties would enable better control of the developing tissue towards the desired structural and compositional endpoints through optimization of the biochemical environment in real time. The objective of this study is to assess the matrix constituents of cartilage using near-infrared spectroscopy (NIRS), a technique that permits full-depth assessment of developing engineered tissue constructs. Mid-infrared (mid-IR) and NIR data were acquired from full-thickness cartilage constructs that were grown up to 4 weeks with and without mechanical stimulation. Correlations were assessed between established mid-IR peak areas that reflect the relative amount of collagen (amide I, amide II, and 1338  $\text{cm}^{-1}$ ) and proteoglycan (PG), (850  $\text{cm}^{-1}$ ), and the integrated area of the NIR water absorbance at 5190  $\text{cm}^{-1}$ . This analysis was performed to evaluate whether simple assessment of the NIR water absorbance could yield information about matrix development. It was found that an increase in the mid-IR PG absorbance at 850  $\text{cm}^{-1}$  correlated with the area of the NIR water peak (Spearman's  $\rho = 0.95$ ,  $p < 0.0001$ ). In the second analysis, a partial least squares method (PLS1) was used to assess whether an extended NIR spectral range (5400–3800  $\text{cm}^{-1}$ ) could be utilized to predict collagen and proteoglycan content of the constructs based on mid-IR absorbances. A subset of spectra was randomly selected as an independent prediction set in this analysis. Average of the normalized root mean square errors of prediction of first-derivative NIR spectral models were 7% for 850  $\text{cm}^{-1}$  (PG), 11% for 1338  $\text{cm}^{-1}$  (collagen), 8% for amide II (collagen), and 8% for amide I (collagen). These results demonstrate the ability of NIRS to monitor macromolecular content of cartilage constructs and is the first step towards employing NIR to assess engineered cartilage in situ.

### Index Headings

Near-infrared spectroscopy; NIR spectroscopy; Fourier transform infrared spectroscopy; FT-IR spectroscopy; Partial least squares; PLS; Multivariate analysis; Cartilage; Tissue engineering

## INTRODUCTION

Articular cartilage cushions diarthrodial bone surfaces and serves as a protective layer against wear but has limited capacity to regenerate and to repair when damaged. Tissue engineering has been employed to attempt to generate cartilage constructs with zonal matrix structure and functional properties similar to those found in native cartilage, but with limited

success to date.<sup>1</sup> An impediment to this effort is that current methods require harvesting at specific time points during in vitro tissue culture experiments to assess cartilage matrix constituents and structure.<sup>2–4</sup> Assays to determine the content of the major cartilage components, collagen and proteoglycans, are routinely performed on harvested, digested tissues.<sup>5–8</sup> Noninvasive assessment would potentially enable better control of engineered cartilage properties towards desired structural and compositional endpoints via conditioning and intervention, as treatments could be customized based on real-time tissue assessments.

Mid-infrared (mid-IR) spectroscopy has been established as a powerful approach for cartilage evaluation,<sup>8–13</sup> including the use of mid-IR fiber optics for intact tissue evaluation<sup>14,15</sup> and IR imaging of engineered cartilage constructs.<sup>16</sup> A limitation of this approach, however, is that the maximum penetration depth of mid-IR radiation into tissue is  $>10\ \mu\text{m}$ , so that its use in situ is restricted to surface evaluation. In contrast, near-infrared spectroscopy (NIRS), which uses shorter wavelength radiation compared to mid-IR, penetrates to a depth of millimeters to centimeters,<sup>17–19</sup> potentially permitting full-depth assessment of developing engineered tissue constructs.

To date, there has been some limited work on the use of NIRS in cartilage analysis, primarily focused on non-specific assessment of water.<sup>20,21</sup> These studies utilized the NIR absorbance between  $7462\text{--}6780\ \text{cm}^{-1}$  (the first OH and CH combination overtones), while other studies that assess skin and hair utilized the NIR water absorbance centered at  $5190\ \text{cm}^{-1}$ .<sup>22,23</sup> The present work extends the use of NIRS to semi-quantitatively assess the matrix constituents of cartilage. Since the primary constituents of cartilage, water, collagen, and proteoglycans (PG) are similar in molecular structure to the primary components of many foods (water, protein, and sugars), we utilized the body of literature related to NIR assessment of food to understand some of the NIR spectral assignments in cartilage.<sup>24–27</sup>

Two separate analyses were performed to test the hypothesis that NIRS is sensitive to macromolecular differences in engineered cartilage. Mid-IR and NIR data were acquired from full-thickness engineered cartilage constructs that were grown with and without mechanical stimulation, an approach that has been widely used to alter the properties of engineered cartilage.<sup>1,28</sup> In the first analysis, correlations were assessed among the well-validated mid-IR peak areas in the  $1700\text{--}850\ \text{cm}^{-1}$  spectral region that reflects the relative amount of collagen and proteoglycan in cartilage<sup>10</sup> and the integrated area of the NIR water absorbance at  $5190\ \text{cm}^{-1}$ . Here we sought to evaluate whether simple assessment of NIR water absorbance could yield information about matrix development. We hypothesized that NIR-determined water content is correlated with PG content. In the second analysis, a partial least squares (PLS1) method was utilized. PLS analysis is a statistical method utilized to find fundamental relationships between predictor and response variables.<sup>29</sup> In this study, PLS was used to assess whether an extended NIR spectral range ( $5400\text{--}3800\ \text{cm}^{-1}$ ) could be utilized to predict relative collagen and proteoglycan content of the constructs that were calculated from mid-IR absorbances. Absorbances in the extended NIR region between  $5400$  and  $3800\ \text{cm}^{-1}$  were used as the predictor variables since they contain matrix constituent signatures of interest for the organic protein, proteoglycan, and water peaks.<sup>24–26</sup> The relationship between the PLS components, which are obtained from the NIR spectra, and the mid-IR absorbances was assessed to evaluate the feasibility of monitoring engineered cartilage construct growth by NIRS.

## MATERIALS AND METHODS

### Engineered Cartilage Constructs

Articular cartilage was harvested from 2–4 week old bovine stifle joints. Chondrocytes were isolated with an 18-h digestion using 0.15% collagenase type II (Worthington Biochemicals

Co., Lakewood, NJ) in Dulbecco's modified eagle's medium (DMEM, Invitrogen, Carlsbad, CA) supplemented with antibiotics (penicillin/streptomycin, Invitrogen, Carlsbad, CA). The digest was filtered through a 100- $\mu\text{m}$  nylon filter after which the isolated chondrocytes were washed twice with phosphate buffered saline (PBS, Invitrogen). Total cell count and viability were determined using the Trypan blue dye exclusion assay.

The isolated chondrocytes were mixed with 0.32% collagen type I gel (Sigma-Aldrich, St. Louis, MO) to yield a final collagen concentration of 0.27% with  $2.5 \times 10^6$  cells/mL. The collagen gel was prepared for cell seeding using the manufacturer's protocol. The cell-collagen constructs were allowed to gel at 37 °C, with full polymerization completed within 35 minutes. Constructs were then cultured within six-well plates in DMEM supplemented with 10% fetal bovine serum (Invitrogen), 2 mM glutamine (Invitrogen), 0.2% penicillin/streptomycin (Invitrogen), 0.25  $\mu\text{g/mL}$  fungizone (Invitrogen), 50  $\mu\text{g/mL}$  gentamicin (Invitrogen), 0.1 mM non-essential amino acids (NEAA), 0.4 mM L-proline (Sigma-Aldrich), and 50  $\mu\text{g/mL}$  L-ascorbic acid-2-phosphate (Sigma-Aldrich). Each construct occupied a single well, had a total volume of 350  $\mu\text{L}$  and was covered with 5 mL of culture medium. Cell culture was performed at 37 °C under a gas mixture of 95% air/5%  $\text{CO}_2$ . The culture media was changed three times per week.

Samples were grown over time up to four weeks, with and without application of ultrasound, to create constructs, also known as spot cultures, with a range of material properties and matrix composition.<sup>30</sup> Pulsed low intensity ultrasound (PLIUS) (Exogen 4000+, Smith & Nephew, Inc., Memphis, TN) at a frequency of 1.5 MHz was applied to the chondrocytes after 72 hours in culture. The ultrasound parameters included a spatial-average temporal-average output intensity of 30  $\text{mW/cm}^2$ , a burst frequency of 1 kHz, and a burst width of 200  $\mu\text{s}$ , with the signal transmitted via coupling gel to the constructs through the bottom of the well plate. Constructs were treated five days per week for 20 min (US-20) or 40 min (US-40). Control constructs were handled identically, including attachment of the ultrasound transducers to the well plate, but the US device was not turned on. There were 16 control, 18 US-20 min, and 15 US-40 min. constructs analyzed in this study.

Full-thickness cartilage constructs were dried at room temperature on a slide for 3 hours to minimize the contribution of bulk water to the NIR spectrum.

### Biochemical Analysis

An additional fourteen control samples with no ultrasound treatment were selected from different time points for biochemical analysis. Constructs were blotted in a consistent fashion for the removal of excess fluid, lyophilized, and digested in 1 mg/mL of Proteinase K (Sigma-Aldrich) in 100 mM of ammonium acetate. Constructs were weighed before and after lyophilization to obtain wet and dry weights. Sulfated glycosaminoglycan (sGAG) content, a measure of total PG content, was quantified from the tissue digests using the colorimetric 1,9-dimethylmethylene blue (DMMB) dye binding assay with a shark cartilage chondroitin sulfate standard.<sup>31</sup>

### Infrared Spectroscopy

A Nicolet Continuum FT-IR Microscope (Thermo Fisher Scientific Inc., Waltham, MA) was used to acquire IR data in transmission mode using a  $100 \times 100 \mu\text{m}$  aperture over the spectral region of 800–6000  $\text{cm}^{-1}$ , which spans both the mid-IR (4000–800  $\text{cm}^{-1}$ ) and NIR (6000–4000  $\text{cm}^{-1}$ ) frequencies with a resolution of 4  $\text{cm}^{-1}$ . For each sample, data acquisition of 64 co-added scans required >15 seconds.

**Mid-Infrared Spectroscopy**—The integrated areas under well-established mid-IR peaks<sup>10</sup> were calculated to assess cartilage macromolecular content. The integrated areas between 1710–1595  $\text{cm}^{-1}$  (amide I), 1590–1500  $\text{cm}^{-1}$  (amide II), and 1338  $\text{cm}^{-1}$  (collagen side chain rotation) correspond to collagen while the peak centered at 850  $\text{cm}^{-1}$  (PG sulfate absorbance) corresponds to PG.<sup>9</sup> The left-hand panel of Fig. 1 shows the characteristic peaks of matrix constituents in representative collagen, aggrecan (the primary PG in cartilage), and cartilage mid-IR spectra. The water absorbance in the mid-IR region, which typically underlies the amide I absorbance, is also shown but was not evaluated in this study.

**Near-Infrared Spectroscopy**—The spectrum of aggrecan has absorbances in the NIR region at 5400 and 4300  $\text{cm}^{-1}$  similar to those identified in aqueous solutions of glucose.<sup>25</sup> The spectrum of collagen has absorbances in the NIR region at 4878 and 4287  $\text{cm}^{-1}$  similar to those used to predict the protein content in milk.<sup>26</sup> The structural bound water was assessed using the integrated area of the NIR band between 5290 and 4990  $\text{cm}^{-1}$ .<sup>32</sup> The right-hand panel of Fig. 1 shows the characteristic peaks of each matrix constituent in representative collagen, aggrecan, water, and cartilage NIR spectra.

## Data Analysis

**Correlations**—Correlations were assessed between integrated areas of mid-IR bands, between biochemically determined S-GAG and the mid-IR PG band, and between the integrated areas of the NIR water band and the mid-IR PG band. Spearman's rho was used to evaluate all correlations. Statistical significance was taken as  $p < 0.05$ .

**Partial Least Squares Models**—PLS1 is a partial least squares regression method that utilizes multiple predictor variables to predict against one response variable.<sup>29</sup> Partial least squares (PLS1) regression was performed using The Unscrambler software (CAMO Software, Oslo, Norway). The NIR spectrum of each sample made up one row of the predictor matrix and the absorbance values at each wavenumber made up the columns of this matrix. A response matrix was created with each calculated mid-IR band area for each sample and was used in decomposing the predictor matrix into components. Once the model was calibrated, the elements of the response matrix were predicted to validate the models.<sup>29</sup> The collagen and PG content of each sample were assessed using the integrated areas of the established mid-IR peaks (Fig. 2), three separate peaks for collagen (amide I, amide II, and the 1338  $\text{cm}^{-1}$  band), and one for PG (850  $\text{cm}^{-1}$  band). A different PLS1 model with a response matrix based on each mid-IR absorbance (amide I and II, 1338  $\text{cm}^{-1}$  and 850  $\text{cm}^{-1}$ ) was developed that employed the variation in the NIR spectral range to predict the corresponding integrated mid-IR peak area, e.g., the concentration of the macromolecule of interest. The NIR region of interest for the current study is shown in the right-hand panel of Fig. 1. The lower frequency endpoint was chosen below the typical cutoff of the NIR range of 4000  $\text{cm}^{-1}$  so that an additional water peak that spans through 3800  $\text{cm}^{-1}$  was included. Therefore, PLS1 models were developed to assess whether the extended NIR spectral range of 5400–3800  $\text{cm}^{-1}$  could be used to predict the relative amount of matrix constituents of engineered cartilage.

## Partial Least Squares-1 Preprocessing, Calibration, Validation, and Prediction

—For each of the four models, three different spectral preprocessing methods were investigated: baseline-corrected, first-derivative, and second-derivative NIR spectra. Multiplicative scattering correction (MSC), which negates amplification and offset artifacts caused by light scattering,<sup>29</sup> was applied when the first and second derivatives of NIR spectra were utilized. Leave-one-out cross-validation was performed on all models. The number of principal components was determined by assessing the unexplained variance plots. These plots show the fraction of the variance in the data that the model cannot explain

as new components are added to the model.<sup>29</sup> Principal components were included until the last significant drop in unexplained variance was observed. Outlier spectra for each model were determined using the Hotelling  $T^2$  ellipse algorithm.<sup>29</sup> Models were calibrated with forty-six to fifty-nine samples, as summarized in Table I. The quality of the fit for each model was assessed by the coefficient of determination of validation ( $R^2$ ) and the root mean square error of prediction (RMSEP).

To quantify the predictive capabilities of our models, sixteen spectra were randomly selected and removed from the models and then used as an independent validation data set. The models were then calibrated by the remaining samples, and the mid-IR peak areas of the 16 validation samples were predicted by PLS1 models. The above procedure was repeated three times with different validation samples and the root mean squares error of prediction values were used to assess performance. Normalized RMSEP was also calculated as the ratio between RMSEP and the range of measured values.<sup>33</sup>

## RESULTS AND DISCUSSION

### Correlations Between Mid-Infrared, Near-Infrared, and Biochemistry Data

The variation of the sample matrix constituents was evident in the mid-IR spectra of the engineered constructs (Fig. 2). Qualitatively, the collagen and PG content varied based on differences in peak heights that arose from growing tissue under diverse conditions. The increase in PG correlated with a decrease in collagen content (Spearman's  $\rho = -0.91$ ,  $p < 0.0001$ ) and with an increase in bound water (Spearman's  $\rho = 0.95$ ,  $p < 0.0001$ ) (Figs. 3 and 4). Although this result supported the hypothesis that water and PG were positively correlated, the negative correlation between PG and collagen was not anticipated. The decrease in total collagen content likely reflects the degradation of the type I collagen scaffold. The statistically significant Spearman's  $\rho$  values signify that simple evaluation of the NIR water band at  $5190\text{ cm}^{-1}$  could be utilized to monitor matrix development. A significant correlation between the PG peak area and the S-GAG values (Spearman  $\rho = 0.6$ ,  $p = 0.026$ ) was also found (Fig. 5). However, the strength of the correlation was weak, likely due to the S-GAG method being volumetric and normalized to wet weight and the IR data having been collected on air-dried samples.

### Partial Least Squares-1 Cross-Validation Analysis

The highest  $R^2$  of validation for prediction of the collagen peak at  $1338\text{ cm}^{-1}$  ( $R^2 = 0.71$ ) was obtained with the model using baseline-corrected spectra, whereas the highest  $R^2$  of validation for the collagen amide I absorbance was obtained with the model using first-derivative spectra ( $R^2 = 0.93$ ). The model using second-derivative spectra yielded the highest  $R^2$  for both the collagen amide II peak area ( $R^2 = 0.92$ ) and the PG peak area at  $850\text{ cm}^{-1}$  ( $R^2 = 0.93$ ). The parameters and  $R^2$  of validation for PLS1 models that utilized the first-derivative spectra are presented in Table I.  $R^2$  values of validation greater than 0.9 were obtained for PLS1 models predicting PG content, amide II, and amide I integrated areas. Figure 6 shows the predicted versus measured plot for the amide I area as an example.

### Partial Least Squares-1 Prediction Analysis: Predicting Constituent Content Using Near-Infrared Spectra

PLS1 models were created to predict collagen and PG content of 16 samples, as described in the Methods section. The normalized root mean square errors of prediction ranged from 9 to 15%. PLS1 models that were based on the first derivative of the NIR spectral range predicted each of the four mid-IR peak areas with smaller errors than models that either used the baseline-corrected spectra or the second derivative of the spectral data, and thus, the parameters as well as  $R^2$  and RMSEP values of the first derivative model are shown in Table

II. For collagen, the models to predict the amide I and amide II integrated areas performed slightly better than the model to predict the 1338  $\text{cm}^{-1}$  peak area (8% normalized RMSEP versus 11%). The model to predict the PG absorbance had a 7% normalized RMSEP. The low normalized RMSEP values obtained in this study indicate that multivariate analysis of NIR data may permit the use of NIR spectroscopy to monitor the macromolecular changes in engineered cartilage.

The current study demonstrates that NIRS can be used to evaluate the matrix constituents of engineered cartilage. Using the gold-standard technique of mid-infrared spectroscopic evaluation of integrated peak areas, increased PG content was shown to correlate with decreased collagen content in the engineered constructs, and the integrated area of the NIR water band centered at 5190  $\text{cm}^{-1}$  strongly correlated with PG content of the constructs. Further, the relative amount of PG and collagen based on the integrated mid-IR bands were predicted using NIR baseline-corrected spectra and their first and second derivatives.

In spite of the differences in optimal methods for preprocessing the data, the NIR data sets were better able to predict collagen with the amide I and amide II peak areas, as compared to the 1338  $\text{cm}^{-1}$  area. We have previously shown that the area of the 1338  $\text{cm}^{-1}$  absorbance is sensitive to cartilage growth and collagen degradation,<sup>15,34</sup> and changes in area of this absorbance may, therefore, be confounded by the presence of the scaffold and the varying developing stages of cartilage. The variable thickness of the spot cultures may also have resulted in variable scattering effects and therefore increased unexplained variance in the models. Nevertheless, the models were as successful in predicting the PG peak area at 850  $\text{cm}^{-1}$ , with comparably high  $R^2$  values, as in predicting the collagen with either the amide I or the amide II peak.

The predictive quality of the multivariate analysis of NIR spectroscopic data can be compared to previous studies that assessed organic contents of food and plants using PLS1 regression. In one study, MSC and second-derivative NIR spectra were utilized to predict the nitrogen and starch content of pine needles by PLS1.<sup>35</sup> In that study, six principal components yielded  $R^2$  values of 0.83 and 0.86, respectively. In another study, PLS1 analysis was employed on NIR data of butter fat content of spreads in order to detect genuine butter fat as opposed to vegetable oils. Five principal components were used and an  $R^2$  value of 0.95 was obtained.<sup>36</sup> PLS1 models predicting the amount of glucose, fructose, sucrose, citric, and malic acids in dry orange juice extracts have been developed using NIR spectra.<sup>37</sup> The model predicting glucose content ( $R^2 = 0.92$ ) had seven principal components and used the first derivative of the NIR spectral range, whereas the model predicting malic acid content ( $R^2 = 0.90$ ) had 22 principal components and used the second derivative of the spectra. Finally, correlations between NIR peaks that are indicative of hydroxyproline, and hence collagen content, and various physical and chemical properties were evaluated using an NIR fiber-optic probe ( $R^2 = 0.75$ ).<sup>27</sup> However, in that study, a multiple linear regression method was employed as opposed to PLS1. In another collagen study, PLS regression on the first derivative of NIR data with one principal component was used to predict the collagen content of bovine meat, but high coefficients of determination were not obtained ( $R^2 = 0.18$ ).<sup>38</sup> We can conclude that the coefficients of determination from the current study are comparable to those obtained in other NIR studies of similar substances.

It is also useful to compare the error of prediction obtained in the PLS1 measurements with the variation within successive biochemical analyses of each engineered cartilage construct performed in this study. The precision of the biochemical DMMB assay, the “gold standard” for PG content evaluation, can vary as a result of different GAG standards of calibration, the nonlinearity in the GAG calibration curve, and the presence of DNA, RNA, and hyaluronan in the sample.<sup>39,40</sup> In the current study, nine repeat biochemical evaluations of each sample

by the DMMB assay yielded coefficient of variation (CV) values ranging from 3 to 14% with a mean of 6%, while repeat measurements of standards used in the calibration curve yielded CVs ranging from 8 to 13% with a mean of 11% (data not shown). The NIR methodology developed in this study is able to predict proteoglycan content (based on integrated areas of the mid-IR bands) with an error of prediction of 7% for PG content, a value comparable to the data spread between repeated biochemical evaluations of the same sample using the DMMB assay.

In addition to being a nondestructive/noninvasive assay, an important advantage of NIR spectroscopy over biochemical assays is the short amount of time required for data collection. Each sample required >15 seconds of scan time in this study, and once a model is developed, the composition prediction can be extremely fast, on the order of minutes or even seconds. The procedure for biochemical assays, on the other hand, requires up to 16 hours to digest the interfering proteins and another 30 minutes after the addition of dimethylmethylene blue.<sup>6</sup> The fact that data acquisition in NIR spectroscopy is rapid will no doubt also be relevant in clinical settings for in situ analysis of cartilage.

Magnetic resonance imaging (MRI) is another modality utilized to noninvasively assess biophysical properties of cartilage matrix. Although some MRI parameters of cartilage have been found to correlate with collagen or GAG content, these parameters have been shown to also be affected by biological and mechanical effects such as hydration and collagen fibril assembly.<sup>41-48</sup> Thus, together, the MR-derived parameters in common use, although sensitive, may not be suitable modalities for assessment of molecular composition either clinically or as a monitor of engineered construct development due to their lack of specificity.

Assessment of cartilage repair tissue obtained through biopsy in the clinical setting<sup>2,3,49</sup> is problematic due to the scarcity of available tissue and the potential morbidity resulting from obtaining samples from the repair site.<sup>50</sup> Visual assessment by arthroscopy is a less invasive alternative, but it provides only a limited description of the tissue. The present work therefore presents a step both toward the use of NIR to assess developing constructs during growth and toward the development of an arthroscopic NIR probe to permit minimally invasive but highly sensitive and specific analysis of the status of developing cartilage matrix.

## Acknowledgments

This study was supported by NIH EB000744, AR056145, and in part by the Intramural Research Program of the NIH National Institute on Aging.

## References

1. Klein T, Malda J, Sah R, Hutmacher D. *Tissue Eng Part B: Rev.* 2009; 15:143. [PubMed: 19203206]
2. Bae D, Yoon K, Song S. *Arthroscopy: J Arthro Relat Surg.* 2006; 22:367.
3. Gooding C, Bartlett W, Bentley G, Skinner J, Carrington R, Flanagan A. *Knee.* 2006; 13:203. [PubMed: 16644224]
4. Yamaoka H, Asato H, Ogasawara T, Nishizawa S, Takahashi T, Nakatsuka T, Koshima I, Nakamura K, Kawaguchi H, Chung U. *J Biomed Mater Res Part A.* 2006; 78:1.
5. Mauck R, Soltz M, Wang C, Wong D, Chao P, Valhmu W, Hung C, Ateshian G. *J Biomechan Eng.* 2000; 122:252.
6. van der Harst M, Brama P, van de Lest C, Kiers G, DeGroot J, van Weeren P. *Osteoarth Cartilage.* 2004; 12:752.

7. Elder B, Vigneswaran K, Athanasiou K, Kim D. *J Neurosurg: Spine*. 2009; 10:623. [PubMed: 19558298]
8. Potter K, Kidder L, Levin I, Lewis E, Spencer R. *Arthritis Rheum*. 2001; 44:846. [PubMed: 11315924]
9. Camacho N, West P, Torzilli P, Mendelsohn R. *Biopolymers*. 2001; 62:1. [PubMed: 11135186]
10. Boskey A, Pleshko Camacho N. *Biomaterials*. 2007; 28:2465. [PubMed: 17175021]
11. David-Vaudey E, Burghardt A, Keshari K, Brouchet A, Ries M, Majumdar S. *Eur Cell Mater*. 2005; 10:51. [PubMed: 16307426]
12. Xia Y, Ramakrishnan N, Bidthanapally A. *Osteoarth Cartilage*. 2007; 15:780.
13. Saarakkala S, Julkunen P, Kiviranta P, Makitalo J, Jurvelin J, Korhonen R. *Osteoarth Cartilage*. 2009; 18:73.
14. Li G, Thomson M, Dicarlo E, Yang X, Nestor B, Bostrom M, Camacho N. *Appl Spectrosc*. 2005; 59:1527. [PubMed: 16390593]
15. West P, Bostrom M, Torzilli P, Camacho N. *Appl Spectrosc*. 2004; 58:376. [PubMed: 15104805]
16. Kim M, Bi X, Horton W Jr, Spencer R, Camacho N. *J Biomed Opt*. 2005; 10:031105. [PubMed: 16229630]
17. Faris F, Thorniley M, Wickramasinghe Y, Houston R, Rolfe P, Livera N, Spencer A. *Clin Phys Physiol Meas*. 1991; 12:353. [PubMed: 1778034]
18. Lammertyn J, Peirs A, De Baerdemaeker J, Nicola B. *Postharvest Biol Technol*. 2000; 18:121.
19. Villringer A, Planck J, Hock C, Schleinkofer L, Dirnagl U. *Neurosci Lett*. 1993; 154:101. [PubMed: 8361619]
20. Spahn G, Plettenberg H, Nagel H, Kahl E, Klinger H, Mückley T, Günther M, Hofmann G, Mollenhauer J. *Med Eng Phys*. 2008; 30:285. [PubMed: 17553725]
21. Hofmann G, Marticke J, Grossstück R, Hoffmann M, Lange M, Plettenberg H, Braunschweig R, Schilling O, Kaden I, Spahn G. *Pathophysiology*. 2009; 17:1. [PubMed: 19481428]
22. Ozaki Y, Miura T, Sakurai K, Matsunaga T. *Appl Spectrosc*. 1992; 46:875.
23. Martin K. *Appl Spectrosc*. 1998; 52:1001.
24. Giangiacomo R. *Food Chem*. 2006; 96:371.
25. Hazen K, Arnold M, Small G. *Appl Spectrosc*. 1994; 48:477.
26. Robert P, Bertrand D, Devaux M, Grappin R. *Anal Chem*. 1987; 59:2187. [PubMed: 3674434]
27. Mitsumoto M, Maeda S, Mitsuhashi T, Ozawa S. *J Food Sci*. 1991; 56:1493.
28. Heath C, Magari S. *Biotechnol Bioeng*. 2000; 50:430. [PubMed: 18626992]
29. Esbensen, K.; Guyot, D.; Westad, F.; Houmoller, L. *Multivariate data analysis: in practice: an introduction to multivariate data analysis and experimental design*. CAMO Process AS; Oslo, Norway: 2002. p. 5
30. Zhang Z, Huckle J, Francomano C, Spencer R. *Ultrasound Med Biol*. 2003; 29:1645. [PubMed: 14654159]
31. De Jong J, Heijs W, Wevers R. *Annal Clin Biochem*. 1994; 31:267.
32. Woo Y, Ahn J, Chun I, Kim H. *Anal Chem*. 2001; 73:4964. [PubMed: 11681473]
33. Dos En S, Popovi D. *IEEE Trans Biomed Eng*. 2008; 55:1973. [PubMed: 18632360]
34. Bi X, Yang X, Bostrom M, Bartusik D, Ramaswamy S, Fishbein K, Spencer R, Camacho N. *Anal Bioanal Chem*. 2007; 387:1601. [PubMed: 17143596]
35. Hiukka R. *Chemom Intell Lab Syst*. 1998; 44:395.
36. Heussen P, Janssen H, Samwel I, Van Duynhoven J. *Anal Chim Acta*. 2007; 595:176. [PubMed: 17605998]
37. Li W, Goovaerts P, Meurens M. *J Agric Food Chem*. 1996; 44:2252.
38. Alomar D, Gallo C, Castaneda M, Fuchslocher R. *Meat Sci*. 2003; 63:441.
39. Zheng S, Xia Y. *Magn Reson Med*. 2010; 63:25. [PubMed: 19918900]
40. Goldberg R, Kolibas L. *Connect Tissue Res*. 1990; 24:265. [PubMed: 2376128]
41. Lin P, Reiter D, Spencer R. *Magn Reson Med*. 2009; 62:1311. [PubMed: 19705467]
42. Potter K, Butler J, Horton W, Spencer R. *Arthr Rheum*. 2000; 43:1580. [PubMed: 10902763]



43. Gray M, Burstein D, Lesperance L, Gehrke L. *Magn Reson Med.* 1995; 34:319. [PubMed: 7500869]
44. Fishbein K, Gluzband Y, Kaku M, Ambia-Sobhan H, Shapses S, Yamauchi M, Spencer R. *Magn Reson Med.* 2007; 57:1000. [PubMed: 17534923]
45. Ramaswamy S, Uluer M, Leen S, Bajaj P, Fishbein K, Spencer R. *Tissue Eng Part C: Methods.* 2008; 14:243. [PubMed: 18620483]
46. Menezes N, Gray M, Hartke J, Burstein D, Professorship E. *Magn Reson Med.* 2004; 51:503. [PubMed: 15004791]
47. Burstein D, Gray M. *Osteoarth Cartilage.* 2006; 14:1087.
48. Li X, Benjamin Ma C, Link T, Castillo D, Blumenkrantz G, Lozano J, Carballido-Gamio J, Ries M, Majumdar S. *Osteoarth Cartilage.* 2007; 15:789.
49. Briggs T, Mahroof S, David L, Flannelly J, Pringle J, Bayliss M. *J Bone Joint Surg.* 2003; 85:1077.
50. Temenoff J, Mikos A. *Biomaterials.* 2000; 21:431. [PubMed: 10674807]

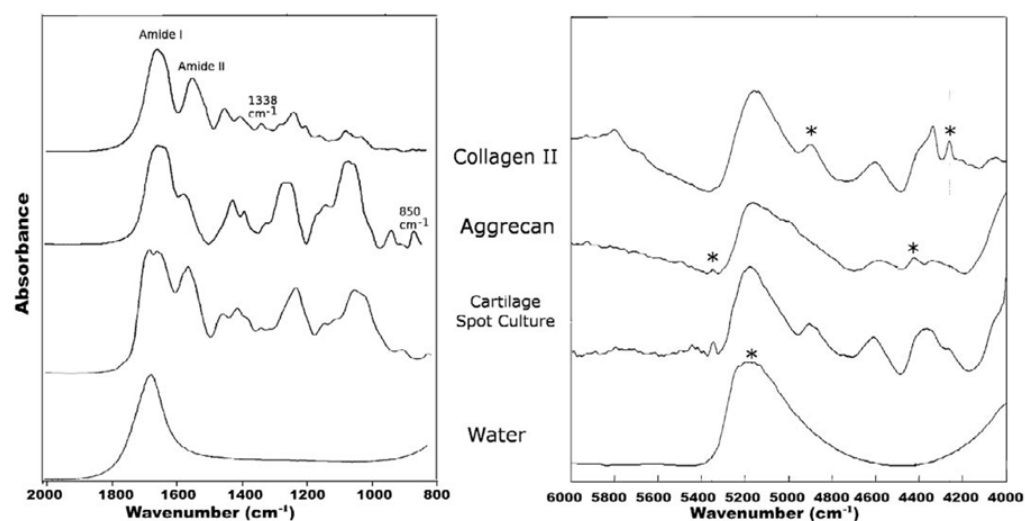


**Fig. 1.** (Left) Mid-IR and (right) NIR spectra of the primary components of articular cartilage. Mid-IR absorbances that arise from collagen (amide I, amide II, and  $1338\text{ cm}^{-1}$ ) and from aggrecan (the primary PG in cartilage,  $850\text{ cm}^{-1}$ ) are labeled. NIR absorbances that are specific to collagen, aggrecan, or water constituents are labeled with asterisks. Both the mid-IR and NIR spectrum of the cartilage spot cultures reflect a combination of the constituent component spectra.

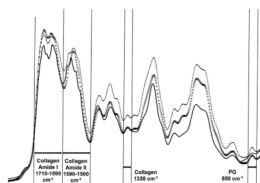


**Fig. 2.** Mid-IR spectra of three representative samples are provided. Three collagen peaks and one PG peak that were used to estimate matrix content are shown. Variation in matrix content of individual samples can be observed based on qualitative peak height differences.

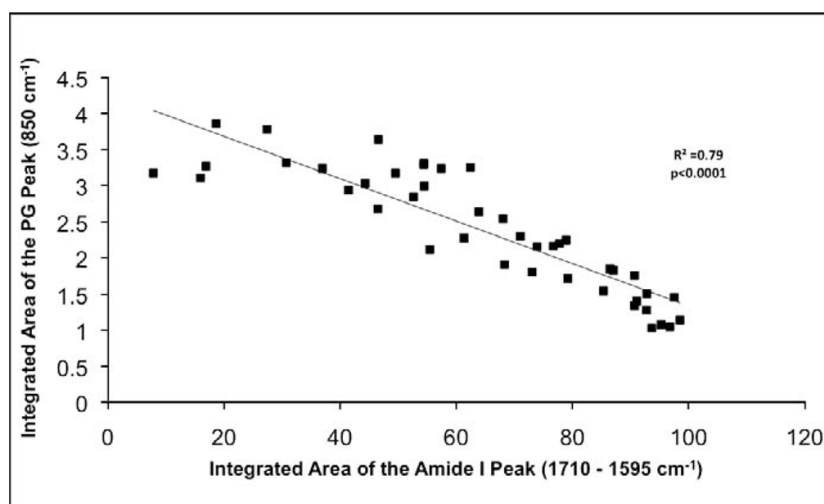


**Fig. 3.** A significant negative correlation between the mid-IR PG peak area and the mid-IR collagen amide I peak area (Spearman's  $\rho = -0.91$ ) was found. The decrease in total collagen content is possibly caused by the degradation of the collagen type I scaffold.

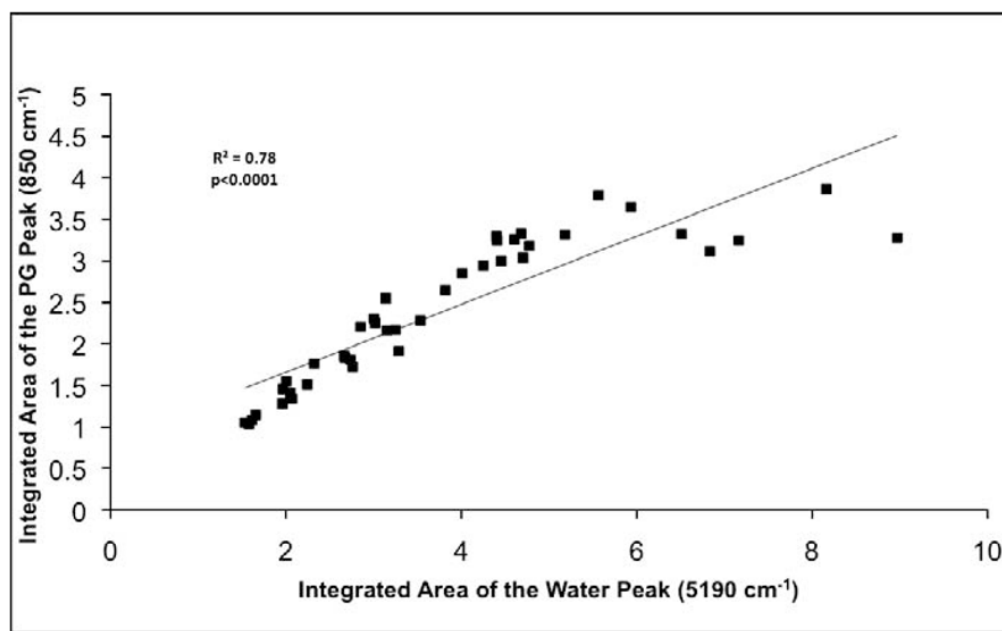


**Fig. 4.** A significant positive correlation was found between the mid-IR PG peak area and the NIR water peak area (Spearman's rho = 0.95).

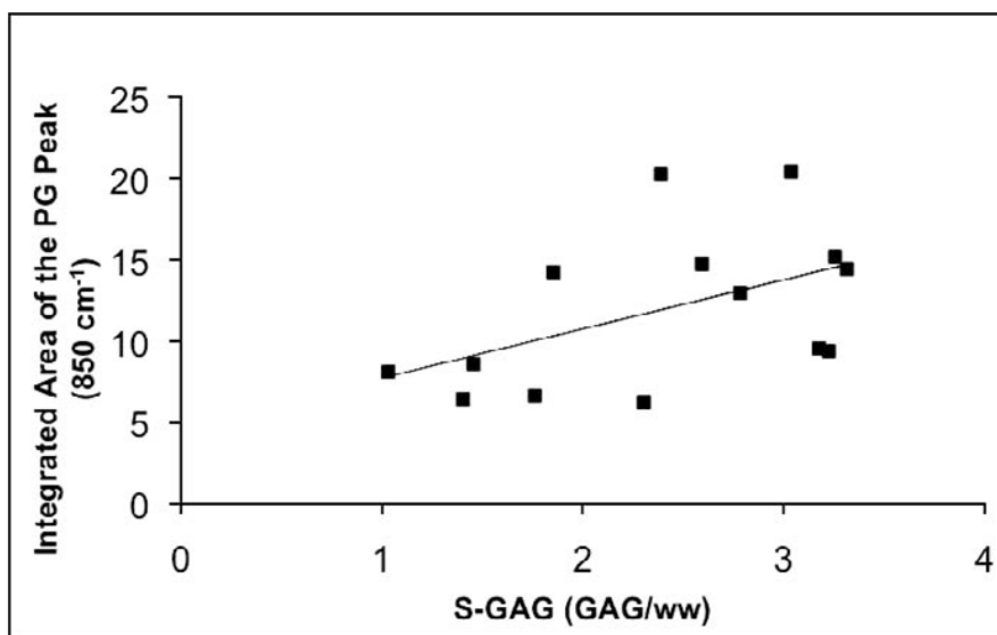


**Fig. 5.** A statistically significant correlation was found between biochemically determined S-GAG content and the mid-IR PG peak area (Spearman's  $\rho = 0.6$ ,  $p = 0.026$ ).

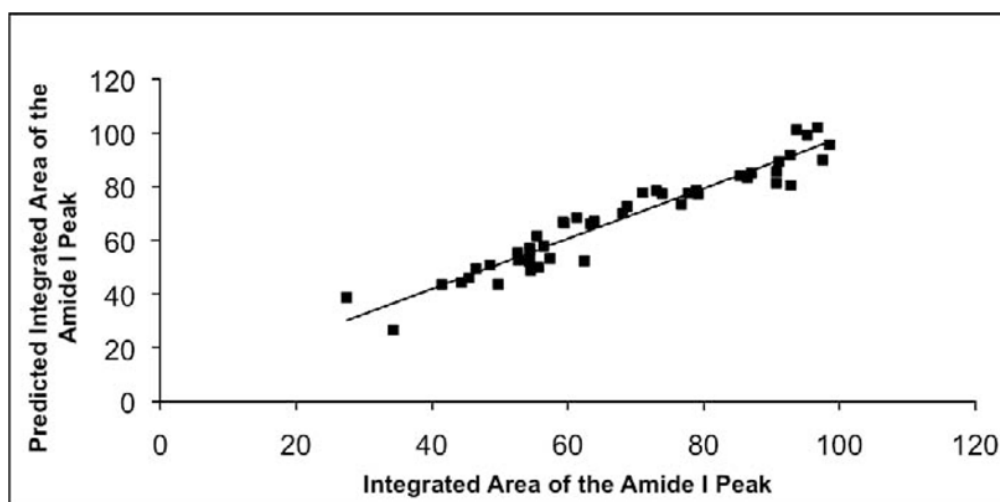


**Fig. 6.** Predicted vs. measured plot of PLS1 cross-validation model. The first derivative of the extended NIR spectral range  $5400\text{--}3800\text{ cm}^{-1}$  was utilized to predict the integrated area of the collagen amide I ( $1710\text{--}1595\text{ cm}^{-1}$ ) absorbance ( $R^2 = 0.93$ ). Three principal components were used.

**TABLE I**

Parameters of PLS1 cross-validation models used to predict mid-IR peak areas. First-derivative NIR spectra were used.

First derivative + MSC	Collagen			
	PG	Amide II		Amide I
	850 cm <sup>-1</sup>	1338 cm <sup>-1</sup>	1590–1500 cm <sup>-1</sup>	1710–1595 cm <sup>-1</sup>
<i>R</i> <sup>2</sup> of validation	0.92	0.58	0.91	0.93
No. of samples	46	55	46	46
Principal components	3	5	2	3
Root mean square error of prediction (integrated absorbance band areas)	0.23	0.32	3.51	5.17



**TABLE II**

Parameters showing the predictive capabilities of PLS1 models used to predict mid-IR peak areas. First-derivative NIR spectra were used.

First derivative + MSC	Collagen			
	PG	Amide II		Amide I
	850 cm <sup>-1</sup>	1338 cm <sup>-1</sup>	1590–1500 cm <sup>-1</sup>	1710–1595 cm <sup>-1</sup>
<i>R</i> <sup>2</sup> of prediction	0.93	0.79	0.90	0.93
Root mean square error of prediction	0.20	0.24	3.60	5.20
Normalized RMSEP	7%	11%	8%	8%
<i>R</i> <sup>2</sup> of calibration	0.93	0.82	0.93	0.92
No. of calibration samples	30	39	30	30
Average no. of principal components from 3 models	2.00	4.67	2.33	1.33